Available online at www.sciencedirect.com

ScienceDirect

Ceramics International 39 (2013) 9085–9089

CERAMICS INTERNATIONAL

www.elsevier.com/locate/ceramint

Microstructure and mechanical properties of C_f/ZrC composites fabricated by reactive melt infiltration at relatively low temperature

Yulin Zhu[a], Song Wang[a,*], Hongmei Chen[a,b], Wei Li[a], Jinming Jiang[a], Zhaohui Chen[a]

[a]*Science and Technology on Advanced Ceramic Fibers and Composites laboratory, National University of Defense Technology, Changsha 410073, China*
[b]*Department of Mechanical Engineering, Hunan International Economics University, Changsha 410205, China*

Received 14 March 2013; received in revised form 22 April 2013; accepted 1 May 2013
Available online 9 May 2013

Abstract

Carbon fiber-reinforced zirconium carbide matrix composites (C_f/ZrC) were prepared by vacuum infiltrating porous carbon/carbon preforms with molten Zr_2Cu alloy at 1200 °C. X-ray diffraction, scanning electron microcopy and transmission electron microscopy analysis were used to characterize the composition and microstructure of the final composites. It was found that the matrix of the composites were composed of the Cu–Zr–C amorphous phase dispersed with either single- or polycrystalline ZrC. Based on the microstructural analysis, the formation mechanism of the matrix was proposed to be a solution-precipitation and grain coalescence process. The influence of the heat treatment at 1800 °C was also investigated. Results indicated that at very high temperature the volatilization of residual metal somewhat deteriorated the flexural strength and the elastic modulus, but the fracture toughness of the composites was improved due to the sintering of ZrC grains.

Keywords: C. Mechanical properties; D. Carbides; Microstructure; Reactive melt infiltration

1. Introduction

Zirconium carbide (ZrC), known as ultra-high temperature ceramics (UHTCs), has attracted increasing attention due to its unique properties, such as extremely high melting point, relatively low density, good solid-state stability [1–3], and excellent ablation resistance at high temperatures [4,5]. This combination of properties makes it potentially useful in applications associated with atmospheric re-entry, hypersonic flight, rocket propulsion, etc. [3,6]. However, ZrC ceramics are brittle and thereby have a tendency toward catastrophic failure [5], which is one of the most crucial problems in their applications. It has been demonstrated effectively to improve the fracture resistance of ZrC by incorporating carbon fibers as reinforcement [6–8].

Owing to its advantages of low cost and capability to produce components with complex geometries [9–12], reactive melt infiltration (RMI) process is known as an attractive technology for creating composite matrixes such as SiC [12,13], HfC [14] and ZrC [6,10,15]. Recently, C_f/ZrC composites are prepared by infiltrating porous C_f/C preforms with either pure Zr [5,8] or Zr-based alloy [16]. Due to the high melting point of these infiltrators, the infiltration process can only be operated at temperatures above 1800 °C, resulting in a great damage to the fibers. Considering that, Zr_2Cu instead of Zr has been used in our previous work to produce C_f/ZrC composites at temperature as low as 1200 °C [6]. However, the formation mechanism of ZrC remains unclear and the effects of the residual melt on microstructure of the composites have not been reported yet.

In this paper, the microstructure of the C_f/ZrC composites prepared by RMI with Zr_2Cu as a reactive infiltrator was studied, and a matrix formation mechanism of the composites was proposed based on the microstructural analysis. Also, the structure and properties of the composites after high temperature treatment were evaluated and investigated in detail.

2. Experimental procedure

The carbon felts were prepared by a needle-punching technique with alternatively stacked 0° weftless piles (T300, an average diameter of about 7 μm, carbon content of 93%

*Corresponding author. Tel.: +86 731 84576441; fax: +86 731 84573165.
E-mail address: wangs_0731@yahoo.cn (S. Wang).

0272-8842/$ - see front matter © 2013 Elsevier Ltd and Techna Group S.r.l. All rights reserved.
http://dx.doi.org/10.1016/j.ceramint.2013.05.004

(impurities of O+H+N+S≤7%), bulk density of 1.76 g cm^{-3}, Toray, Japan), short-cut-fiber webs and 90° weftless piles. The fiber volume is about 30 vol%. The protective carbon layer outside the carbon fibers was fabricated by the CVD process, which was operated at 900–1150 °C with C_3H_6 as the reactant gas and N_2 the dilute gas.

In order to prepared porous C_f/C performs, The as-obtained felts were firstly infiltrated with ethanol/phenolic resins solution (with a weight ratio of 1:1) under a mild vacuum of about 20 Pa; after dwelling there for 6 h, the saturated felts were then cured at 80 °C for 4 h and at 150 °C for 3 h; finally, the cured felts were pyrolyzed at 1200 °C for 60 min in N_2 (purity≥ 99.999 vol%, O_2+H_2O≤0.001 vol%) and atmospheric pressure, with a heating rate of 10–15 °C/min.

The preparation of C_f/ZrC composites included stages as follows: the Zr_2Cu alloy (purity≥99.2 wt%, impurities (Hf+Fe +Ti+Si+Mg+Al+Ni)≤0.8 wt%; Hunan Rare Earth Metal & Material Institute, Hunan, China) was rapidly heated up to 1200 °C in vacuum. After the alloy melted completely, the porous C_f/C preforms were mechanically driven into the melt and kept there for 2 h, and then separated from the liquid Zr_2Cu bath and cooled spontaneously to room temperature. Some specimens were further treated at 1800 °C for 2 h in vacuum, with a heating rate of 10 °C/min, and then cooled at 7.5 °C/min to 800 °C. The excess adhering solidified melt was removed from the sample by the grinding machining with diamond wheel.

The volume fractions of the solid phases were measured by ICP and chemolysis, according to the theoretical densities of 6.63 g cm^{-3} for ZrC, 1.55 g cm^{-3} for deposited C, 8.96 g cm^{-3} for Cu, 6.49 g cm^{-3} for Zr and 1.76 g cm^{-3} for T300 fiber, which was described previously [6,17]. The phases were analyzed by X-ray diffraction with a Bruker D8 Advance instrument. The microstructures were observed by scanning electronic microscopy (SEM, Quanta-200) with accessorial energy-dispersive spectroscopy (EDS). The TEM sample was prepared by grinding a bulk sample to about 80 μm in thickness and then a 3 mm diameter disc was cut out. The disc was subsequently dimpled and ion milled. Images and selected area electron diffraction (SAED) pattern were obtained with a transmission electron microscope (TEM; JEOL, Tokyo, Japan; JEM-2010F). Image analysis software package (Image J, National Institutes of Health, Bethesda, MD) was used to determine average fibers diameter and phases content of the composites, by measuring at least 10 different backscattered electron images and 30 fibers per image.

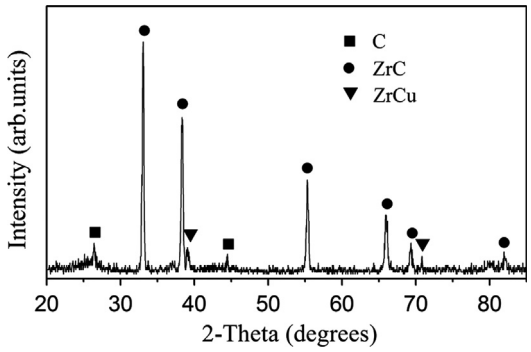

Fig. 1. XRD pattern of the C_f/ZrC composites.

Flexural strength was measured using a three-point-bending test on five specimens of 3.0 mm × 4.0 mm × 60 mm with 50 mm span and a crosshead speed of 0.5 mm min^{-1} (Model 5566, Instron Corp., High Wycombe, UK). Fracture toughness was evaluated by a single-edge notched-beam test with a 24 mm span and a crosshead speed of 0.05 mm min^{-1}, and three samples were tested. The test bars, 3.0 mm × 6.0 mm × 40 mm, were notched by electromachining with a 0.2-mm-diameter Mo line. The notches were about 0.2 mm in width and 3.0 mm in depth. All samples were gotten by the electric discharge machining. They were ground, polished with a series of diamond pastes to a surface finish of 0.5 μm, and beveled the edges.

3. Results and discussion

The XRD pattern of the obtained C_f/ZrC composites is shown in Fig. 1. The main phases existing in the composite are carbon, ZrC, and ZrCu. The phase contents determined by ICP and chemolysis are listed in Table 1, which reveals that the generated ZrC is the major phase in the composites. Therefore, it can be indicated that the present process is an efficient approach to yield ZrC ceramic.

Since the reaction between C (molar volume V_C=7.7 cm^3/mol) and molten Zr with the formation of ZrC (molar volume V_{ZrC}=15.6 cm^3/mol) leads to a volume increase of 200%, all of the superfluous melt could be squeezed from the composites owing to solid volumetric expansion. However, a small quantity of ZrCu compound (with a content of 8.3 ± 1.7 vol%) was detected (Fig. 1), implying that the consumption of Zr element was not complete. On the one hand, Cu additive greatly decreased the infiltrating temperature and consequently slowed

Table 1
Compositions of the C_f/ZrC composites before and after heat treatment.

Specimens	Open porosity (%)	Volume fractions of phases (vol%)				
		C-fiber	ZrC	C	Residual metallic alloys	
					Zr (vol%)	Cu (vol%)
As-received	6.9 ± 1.2	31.9 ± 2.7	43.8 ± 2.1	7.0 ± 1.9	2.9 ± 0.4	7.5 ± 1.2
1800 °C, vacuum	12.7 ± 1.6	31.9 ± 2.7	45.2 ± 1.8	6.4 ± 1.4	0.7 ± 0.8	3.1 ± 0.8

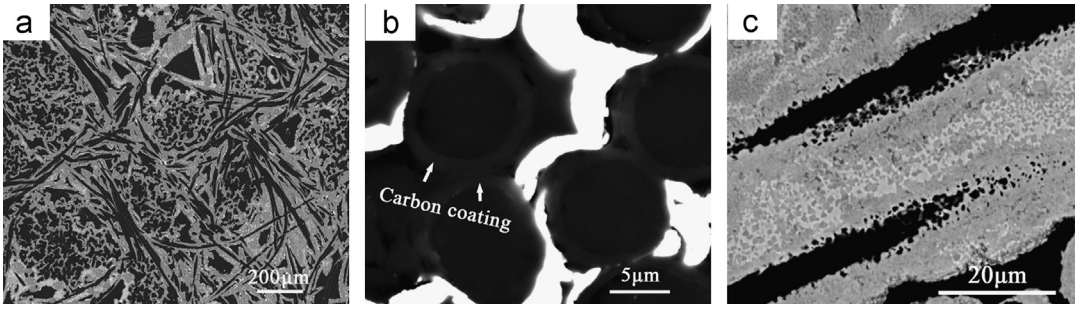

Fig. 2. SEM micrographs of (a) representative cross-section, (b) fiber section and (c) matrix of the C_f/ZrC composites.

down the speed of Zr–C reaction. For the other, because of the absence of the Cu_xC_y [18], Cu played a role of diluting agent to reduce the reactant concentrations in the melt, depressing the conversion of Zr and C to form ZrC.

A representative cross-section of the C_f/ZrC composites is shown in Fig. 2a. It can be seen that the composites have a dense structure with a relatively homogeneous phase distribution. The morphology of fibers is shown in Fig. 2b, which exhibits an intact section surrounded by carbon coating. Determined by image analysis, the fibers have an average diameter of 6.9 ± 0.2 μm, nearly equal to the raw value. Therefore, due to the existence of CVD-carbon layer, the fibers were effectively protected from being eroded by the liquid metal.

The morphology of the matrix is shown in Fig. 2c, which reveals that lots of micron-sized particles are dispersed within a continuous phase. EDS analysis certified that these particles were enriched in C and Zr, and the surrounding phase was comprised of 16 at% C, 16 at% Zr and 68 at% Cu. Image analysis further determines that the particles have an average content of 45.1 ± 2.8 vol%, very close to the measured ZrC content listed in Table 1. Together with the XRD results shown in Fig. 1, it is believed that the particles are ZrC grains and the surrounding is residual Cu-enriched phase.

Additionally, a dispersed structure was detected at the edge of the carbon matrix, suggesting a dissolution process of carbon into the melt. Furthermore, with increasing distance from the deposited carbon, the formed ZrC grains decrease gradually, resulting in a sparse distribution in the central area. These features, combined with the presence of the isolated carbide crystallites in the metal phase, indicate that the formation of ZrC is controlled by the solution-precipitation mechanism [5,19], i.e. carbon dissolves into alloy liquid and diffuses toward lower concentration area. Then ZrC precipitates from the supersaturated solution. The concentration gradient forms during the diffusion process and consequently causes a non-uniform ZrC distribution in the melt.

The matrix was magnified to observe the details in Fig. 3a, which shows that the ZrC grains have platelet shapes and disorderly orientations, and some of them coalesce together to form an unusually larger particle. The inner microstructure of the ZrC particle is shown in Fig. 3b. Numbers of nanoscale inclusions can be found inside the ZrC matrix. TEM and EDS analyses further reveal that these inclusions concentrate along the grain boundaries and are composed of Cu, Zr and C (Fig. 3c and d). According to the similar phenomena reported in Ref. [5], the inclusions are Cu–Zr–C eutectics, which are trapped during the process of grains coalescence. Compared with the C_f/ZrC composites prepared with pure Zr infiltrator at 1900 °C [5], the present composites have much less eutectic inside the ZrC matrix, which might be ascribed to the dilution effect of Cu additive as well as relative low infiltrating temperature.

Besides the micron-sized ZrC particles, nano-sized grains were produced. A TEM bright-field image (Fig. 4a) was taken of the aforementioned continuous phase, which revealed that many nano-sized pellets with homogeneous dimension distributed in the melt, and some of them began to coalesce with others. SAED pattern taken of these pellets showed a spot pattern overlaid with homocentric rings, with radiuses corresponding to characteristic of polycrystalline ZrC (Fig. 4b). High resolution TEM (HRTEM) image revealed that the residual melt was amorphous (Fig. 4c). It can be inferred that these nano-sized polycrystals are produced at the initial stage of ZrC growth.

Based on the above characterization results, the following matrix formation mechanism of the C_f/ZrC composites was deduced. At the beginning of RMI, solid carbon dissolved into Zr_2Cu melt since they had contacted with each other, and then ZrC nuclei were formed and precipitated from the metallic solution, and then developed into nano-sized polycrystalline ZrC. During the further growth, some crystals coalesced together accompanying by a capture of liquid melt inside the ZrC matrix.

A heat treatment was conducted to investigate the effects of the residual melt on structure and properties of the final composites. The cross-section of the C_f/ZrC composites heat-treated at 1800 °C for 2 h in vacuum is shown in Fig. 5a and b. A few small pores can be found in the composites as well as on the surface of the grains. Meanwhile it can be seen from Table 1 that both the Cu and Zr contents decreased after treatment. According to Zhang et al. [20], the Cu-enriched melt is evaporable at high temperature in vacuum, due to its high saturated vapor pressure. Therefore, those pores might be caused by the volatilization of residual metal. However, the carbon fibers seemed to keep the initial diameter, indicating that the treatment had little scathe on the fibers.

The mechanical properties of the C_f/ZrC composites before and after treatment are listed in Table 2. After high temperature

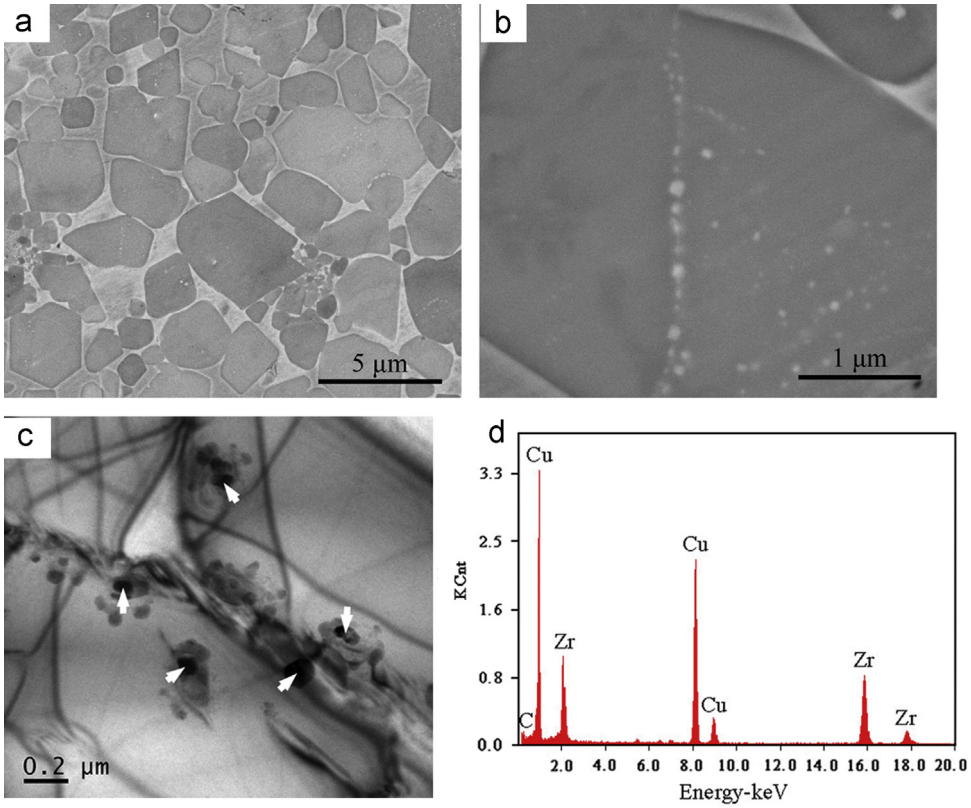

Fig. 3. SEM micrographs of (a) ZrC grains in the matrix of the composites, (b) nano-scale inclusions inside the grains, (c) TEM bright-field image and (d) EDS pattern of the inclusions.

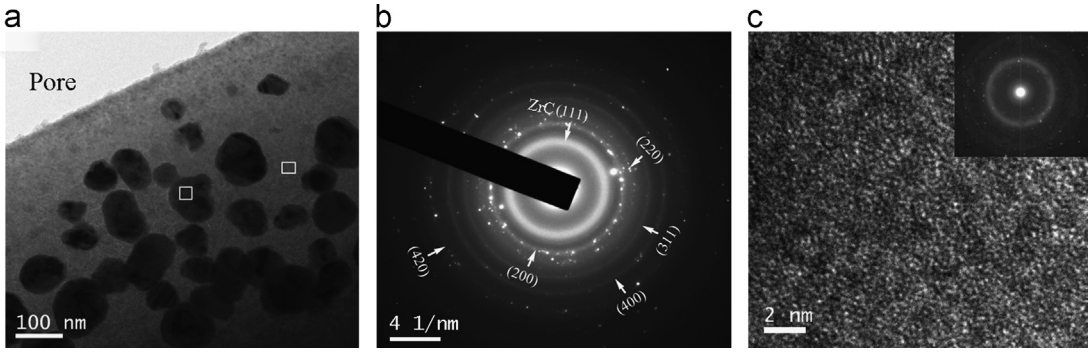

Fig. 4. (a) TEM bright-field image of nano-sized particle dispersed within the residual melt, (b) SAED pattern from the particle, and (c) HRTEM image of the residual melt.

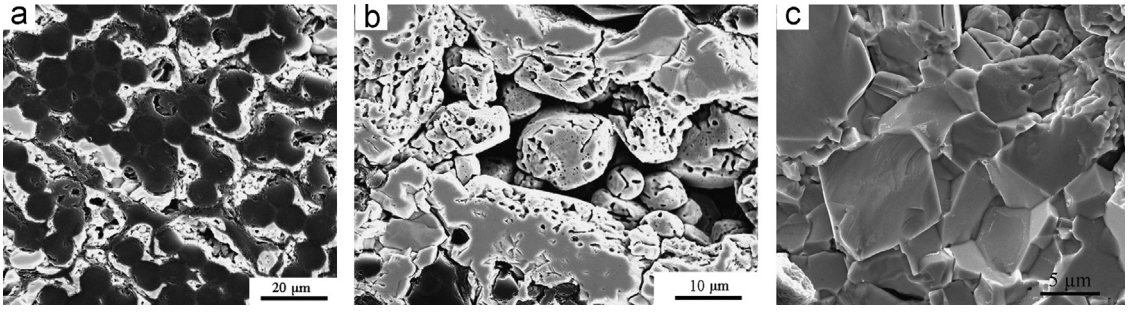

Fig. 5. SEM micrographs of (a) cross-section, (b) surfaces of the ZrC grains, and (c) fracture surface of the C_f/ZrC composites after heat treatment at 1800 °C for 2 h in vacuum.

Table 2
Mechanical properties of the C_f/ZrC composites before and after heat treatment.

Specimens	Flexural strength (MPa)	Elastic modulus (GPa)	Fracture toughness (MPa $m^{1/2}$)
As-received	120.4 ± 2.8	68.7 ± 3.3	6.9 ± 0.5
1800 °C, vacuum	104.7 ± 3.2	58.8 ± 1.9	8.7 ± 0.7

treatments, the flexural strength and elastic modulus of the composites decreased. The reason might be mainly ascribed to the formation of pores, since they can greatly weaken the capacity of matrix to transfer load. Although the ZrC grains exhibited porous surfaces, a compact inner texture could still be detected in the fracture surface of the treated composites (Fig. 5c). Meanwhile, most ZrC grains began to sinter when the annealing temperature increased to 1800 °C. These might be the reasons why the composites had higher fracture toughness.

4. Conclusions

C_f/ZrC composites were prepared by vacuum infiltrating C_f/C preforms with molten Zr_2Cu alloy at 1200 °C. Microstructure and mechanical properties of the composites were investigated. The results revealed that the matrix was composed of ZrC dispersed within a Cu–Zr–C amorphous phase. ZrC as the main constituent was either single- or polycrystalline. Based on the microstructural analysis, a matrix formation mechanism was proposed. The influence of the heat treatment at 1800 °C was also investigated. The losses of flexural strength and elastic modulus after treatment were caused by the volatilization of residual metal. And the improvement of fracture toughness was ascribed to the sintering of ZrC grains.

Acknowledgments

The authors are grateful to National Natural Science Foundation of China (51002186 and 90916002) for financial support. In addition the authors are grateful to Aid Program for Innovative Group of National University of Defense Technology and Aid Program for Science and Technology Innovative Research Team in Higher Educational Institutions of Hunan Province.

References

[1] D. Sciti, S. Guicciardi, M. Nygren, Spark plasma sintering and mechanical behaviour of ZrC-based composites, Scripta Materialia 59 (2008) 638–641.
[2] S.N. Karlsdottir, J.W. Halloran, Rapid oxidation characterization of ultra-high temperature ceramics, Journal of the American Ceramic Society 90 (2007) 3233–3238.
[3] S.M. Zhang, S. Wang, Y.L. Zhu, Z.H. Chen, Fabrication of ZrB_2–ZrC-based composites by reactive melt infiltration at relative low temperature, Scripta Materialia 65 (2011) 139–142.
[4] W. Sun, X. Xiong, B.Y. Huang, G.D. Li, H.B. Zhang, Z.K. Chen X.L. Zheng, ZrC ablation protective coating for carbon/carbon composites, Carbon 47 (2009) 3368–3371.
[5] L.H. Zou, N. Wali, J.M. Yang, N.P. Bansal, Microstructural development of a C_f/ZrC composite manufactured by reactive melt infiltration, Journal of the European Ceramic Society 30 (2010) 1527–1535.
[6] Y.L. Zhu, S. Wang, W. Li, S.M. Zhang, Z.H. Chen, Preparation of carbon fiber-reinforced zirconium carbide matrix composites by reactive melt infiltration at relative low temperature, Scripta Materialia 67 (2012) 822–825.
[7] D. Zhao, C.R. Zhang, H.F. Hu, Y.D. Zhang, Ablation behavior and mechanism of 3D C/ZrC composite in oxyacetylene torch environment, Composites Science and Technology 71 (2011) 1392–1396.
[8] Y.G. Wang, X.J. Zhu, L.T. Zhang, L.F. Cheng, Reaction kinetics and ablation properties of C/C–ZrC composites fabricated by reactive melt infiltration, Ceramics International 37 (2011) 1277–1283.
[9] W.B. Hillig, Melt infiltration approach to ceramic matrix composites, Journal of the American Ceramic Society 71 (1988) C-96–C-99.
[10] S.M. Zhang, S. Wang, W. Li, Y.L. Zhu, Z.H. Chen, Microstructure and properties of W–ZrC composites prepared by the displacive compensation of porosity (DCP) method, Journal of Alloys and Compounds 509 (2011) 8327–8332.
[11] D.W. Lipke, Y. Zhang, Y. Liu, B.C. Church, K.H. Sandhage, Near net-shape/net-dimension ZrC/W-based composites with complex geometries via rapid prototyping and displacive compensation of porosity, Journal of the European Ceramic Society 30 (2010) 2265–2277.
[12] J.N. Ness, T.F. Page, Microstructural evolution in reaction-bonded silicon carbide, Journal of Materials Science 21 (1986) 1377–1397.
[13] N.R. Calderon, M. Martínez-Escandell, J. Narciso, F. Rodríguez-Reinoso, The combined effect of porosity and reactivity of the carbon preforms on the properties of SiC produced by reactive infiltration with liquid Si, Carbon 47 (2009) 2200–2210.
[14] Y. Liu, D.W. Lipke, Y. Zhang, K.H. Sandhage, The kinetics of incongruent reduction of tungsten carbide via reaction with a hafnium–copper melt, Acta Materialia 57 (2009) 3924–3931.
[15] M.B. Dickerson, P.J. Wurm, J.R. Schorr, W.P. Hoffman, P.G. Wapner, K.H. Sandhage, Near net-shape, ultra high melting, recession-resistant ZrC/W-based rocket nozzle liners via displacive compensation of porosity (DCP) method, Journal of Materials Science 39 (2004) 6005–6015.
[16] Y.G Tong, S.X. Bai, K. Chen, C/C–ZrC composite prepared by chemical vapor infiltration combined with alloyed reactive melt infiltration, Ceramics International 38 (2012) 5723–5730.
[17] S. Nafisia, R. Coxb, R. Ghomashchi, Laser ablation ICP-MS investigation of solute element distributions during Al–Si solidification, Journal of Alloys and Compounds 415 (2006) 99–105.
[18] T.B. Massalski, H. Okamoto, P.R. Subramanian, L. Kacprzak, in: Binary Alloy Phase Diagrams, second edition, ASM International Materials Park, Ohio, 1990.
[19] M.X. Zhang, B. Huang, Q.D. Hu, J.G. Li, Study of formation behavior of ZrC in the Cu–Zr–C system during combustion synthesis, International Journal of Refractory Metals and Hard Materials 31 (2012) 230–235.
[20] S.M. Zhang, S. Wang, W. Li, Y.L. Zhu, Z.H. Chen, Mechanical properties of the low-temperature reactive melt infiltrated ZrB_2–ZrC based composites, Materials Letters 78 (2012) 81–84.